Journal of Computational Physics 229 (2010) 3502–3522

Contents lists available at ScienceDirect

Journal of Computational Physics

journal homepage: www.elsevier.com/locate/jcp

Numerical solution of certain classes of transport equations in any dimension by Shannon sampling

Romina Gobbi, Silvia Palpacelli, Renato Spigler *

Dipartimento di Matematica, Università "Roma Tre", 1 Largo S. Leonardo Murialdo, 00146 Rome, Italy

ARTICLE INFO

Article history:
Received 20 February 2009
Received in revised form 9 November 2009
Accepted 13 January 2010
Available online 20 January 2010

MSC:
65M25
65M70
65N35
65T60
94A20
35L60

Keywords:
Nonlinear transport equations
Integro-differential hyperbolic equations
Characteristics
Shannon sampling
Shannon wavelets

ABSTRACT

A method is developed for computing solutions to some class of linear and nonlinear transport equations (hyperbolic partial differential equations with smooth solutions), in any dimension, which exploits Shannon sampling, widely used in information theory and signal processing. The method can be considered a spectral or a wavelet method, strictly related to the existence of characteristics, but allows, in addition, for some precise error estimates in the reconstruction of continuous profiles from discrete data. Non-dissipativity and (in some case) parallelizability are other features of this approach. Monotonicity-preserving cubic splines are used to handle nonuniform sampling. Several numerical examples, in dimension one or two, pertaining to single linear and nonlinear (integro-differential) equations, as well as to certain systems, are given.

1. Introduction

In this paper, we develop a method for computing solutions to some class of linear and nonlinear transport equations, i.e. hyperbolic partial differential equations (PDEs) with smooth solutions, in any dimension. Such a method exploits the celebrated Shannon sampling theorem, widely used in the field of information theory, in particular in telecommunications and signal processing. It can be considered essentially as a spectral method, strictly related to the existence of characteristics, and moreover has the attractive feature of representing, at any time, the unknown (sought) solution as a superposition of elementary distributions (delta functions). It consists of taking a suitable number of sampled values of the initial profile, solving then a related system of ordinary differential equations (ODEs), and reconstructing the continuous solution at any chosen time $t > 0$ through the so-called *sinc* or cardinal functions [25,16,12,20,22,23]. This method can also be considered a wavelet method, since the *sinc* functions are wavelets (the Shannon wavelets), but we use them only in the reconstruction, made according to Shannon (or Whittaker–Shannon–Kotel'nikov) sampling theorem, e.g. see [28]. Incidentally, observe that since the *sinc* kernels decay slowly, such expansions are often avoided. However, a "fast *sinc* transform" does exist, which

* Corresponding author. Tel.: +39 06 5733821; fax: +39 06 57338080.
E-mail address: spigler@mat.uniroma3.it (R. Spigler).

0021-9991/$ - see front matter © 2010 Elsevier Inc. All rights reserved.
doi:10.1016/j.jcp.2010.01.013

exploits the nonuniform fast Fourier transform (NUFFT), and whose cost is comparable to that of the FFT [10]. De la Vallée Poussin seems to have been the first who introduced this kind of interpolation [5]; nice reviews about this subject can be found in [1,7,11,23,14,18].

It is remarkable that, according to Shannon theorem, the reconstruction through the *sinc* interpolation of a band-limited function, i.e. a function whose Fourier transform has a bounded support, can be virtually error free. By the celebrated Paley–Wiener theorem, for instance, any entire function of exponential type which belongs to $L^2(\mathbf{R})$ has an L^2 Fourier compactly supported transform [13]. The reconstruction is guaranteed provided that a sufficiently high number of "samples" is taken. In our method, numerical errors come in, of course, evaluating the various samples, which are obtained upon numerical integration of the ODEs governing the characteristics. Needless to say that the possibility of reducing the numerical solution of the given PDE to that of a family of ODEs offers several advantages,such as the choice of highly sophisticated ODE integrators. In addition, since it avoids spatial discretization, this method turns out to be *non-dissipative*, and is in some cases *parallelizable*. We compared the results obtained by an explicit fourth-order Runge–Kutta solver with those computed by the "optimal" third-order TVD Runge–Kutta scheme, observing negligible differences. Compared to the classical method of characteristics, however, the present Shannon-based sampling approach allows, in principle, to solve the aforementioned ODEs without introducing any interpolation error, and the minimum number of samples needed for the full reconstruction of the solution can be estimated precisely. Comments on the numerical errors of various kind are made below, in Section 2.

The hyperbolic equations to which this method can be applied are scalar equations but in any dimension, possibly nonlinear, nonlocal, and singular at the boundaries [8]), as well as certain systems. In this paper, we assume that they possess smooth solutions, in particular that they have no shocks (for such a reason we refer to them as to "transport equations").

Shannon sampling has been extensively used in the field of signal processing, in modern telecommunication theory, but also in a few other areas of numerical analysis, such as interpolation, e.g. see [22,23,7]. It has also been used to solve certain PDEs, but upon reduction of them to integral equations, e.g. see [21].

In Section 2, we present the general ideas about the method. In Section 3, we introduce some additional ingredients, related to the nonuniformity of the samples distribution. In fact, "shape preserving" cubic splines have been used. In Section 4, some numerical examples in 1D are given, in Section 5 the method and related examples pertaining to 2D problems are presented, while in Section 6 the same is done for some systems of PDEs. In Section 7, finally, the high points of the paper are summarized.

2. Generalities

The so-called Whittaker–Shannon–Kotel'nikov theorem, or simply Shannon sampling theorem, states that, if a function f is *band-limited* to $[-\pi W, +\pi W],\ W > 0$, i.e. it belongs to $L^2(\mathbf{R}) \cap C^0(\mathbf{R})$ and its Fourier transform vanishes outside the interval $[-\pi W, +\pi W]$, so that it can be represented as

$$f(x) = \int_{-\pi W}^{+\pi W} e^{-ix\xi} \widehat{f}(\xi) d\xi \tag{1}$$

for some function $\widehat{f} \in L^2((-\pi W, +\pi W))$, then it can be reconstructed, i.e. fully recovered, from its samples $f(k/W)$, taken at evenly spaced points, $x_k := k/W,\ k \in \mathbf{Z}$. This is done through the interpolation formula

$$f(x) = \sum_{k=-\infty}^{+\infty} f\left(\frac{k}{W}\right) \frac{\sin[\pi(Wx-k)]}{\pi(Wx-k)} =: \sum_{k=-\infty}^{+\infty} f\left(\frac{k}{W}\right) sinc(Wx-k), \tag{2}$$

where the cardinal or *sinc* function, $sinc\, x := \frac{\sin(\pi x)}{\pi x}$ appears, and the series in (2) converges absolutely and uniformly on compact subsets of the real line [1,28]. Note that here the step-size in the interpolation is $h := 1/W$.

In this paper, we apply the idea of the Shannon sampling to solutions of certain evolutionary partial differential equations, say $u(x,t)$. We consider them as "signal" but as functions of space, x, for fixed times. "Finite duration" or "time-limited" signals will refer therefore to functions compactly supported in space, $t \geqslant 0$ being fixed. For a full, exact reconstruction, signals may have an infinite duration, but should be band-limited, and the sampling frequency should be equal to or larger than the Nyquist frequency, which in the present notation is W; hence one should take $h \leqslant 1/W$. Clearly, when the signal has an infinite duration, infinitely many equally spaced samples should be taken, and in practice this would imply a *truncation error* as the series in (2) must be necessarily terminated. Also, the *sinc* kernel decays slowly, hence the series in (2) converges slowly, to the point that errors in samples amplitudes might result in divergence. A good way to circumvent such a difficulty is "oversampling", i.e. using a sampling frequency $\lambda\pi W$ with $\lambda > 1$ instead of πW, see [4].

In our examples below, we have compactly supported initial values $u(x,0)$, say, e.g. in 1D, on some interval $[0, L]$, and also the solution $u(x,t)$ will be compactly supported at every time $t > 0$. Hence, a finite number of samples, N, larger than $2\pi WL$, suffices. However, the requirement of being band-limited cannot be satisfied when the signal has a finite duration. Much research has been devoted to this case, which gives rise to the so-called *aliasing error*. A useful result is the following: If $f \in L^2(\mathbf{R}) \cap C^0(\mathbf{R})$ is such that its Fourier transform is $\widehat{f} \in L^1(\mathbf{R})$, then the estimate

$$|f(x) - (S_W f)(x)| \leqslant \sqrt{\frac{2}{\pi}} \int_{|\xi| \geqslant \pi W} |\widehat{f}(\xi)| d\xi, \tag{3}$$

holds, where $(S_W f)(x)$ denotes the series in (2), "called the sampling series of f", e.g. see [1]. This means that f can be approximated uniformly by the sampling series $S_W f$. In (3) there is an upper bound for the error made taking $S_W f$ in place of f, and it has been shown that such an estimate is optimal since the constant $\sqrt{2/\pi}$ cannot be improved [1]. Clearly, when f is band-limited (to the interval $[-\pi W, +\pi W]$), the previous formula reduces to the usual one, i.e. the approximation being discussed yields the exact result [1].

In addition to the truncation error and the aliasing error, the signal reconstruction may be affected by other errors, such as, e.g. roundoff of the sample amplitudes and imperfect nodes, k/W [15,24]. In signal processing, roundoff may be due to quantization, while for us it may be due to the numerical error made by the ODE integrators.

On the other hand, every given scalar hyperbolic equation, in any dimension, admits of characteristics. These are a family of solutions to a related ODE system, whose size equals the dimension above, and the PDE itself becomes a (scalar) ODE on each characteristic.

The class of equations to which we shall apply the Shannon sampling, is given by

$$\partial_t u + \nabla_x \cdot f(u; x, t) = c(x, t)u + s(x, t), \quad x \in D \subseteq \mathbf{R}^d, \;\; t > 0, \tag{4}$$

where u is scalar, and

$$f(u; x, t) := [a(x, t)g(\mathcal{I}[u]) + b(x, t)]u, \tag{5}$$

$g(\cdot)$ being a possibly *nonlinear* function of its argument, $\mathcal{I}[u]$, where

$$\mathcal{I}[u](t) := \int_{\mathbf{R}^d} \mathcal{K}(\xi)u(\xi, t)d\xi. \tag{6}$$

We assume for simplicity that all coefficients are smooth functions. More general forms could be considered. For instance, on the right-hand side of (5), a term like $\alpha(x, t)$ could be added, which amounts to change the source term, $s(x, t)$, in (4). Similarly, adding a term like $\beta(\mathcal{I}[u])$ or letting g depend on x and t as well. Moreover, g could be replaced by a possibly nonlinear function of m arguments like $\int_{\mathbf{R}^d} \mathcal{K}_i(x')u(x', t)dx'$, for $i = 1, 2, \ldots, m$. Finally, the kernel $\mathcal{K}(x')$ (or the kernels $\mathcal{K}_i(x')$) may be let also depend on x and t. Clearly, suitable supports of such kernels may reduce the domain of integration to a smaller (bounded or unbounded) one, and in particular letting the integral act on a lower dimensional space, $\mathbf{R}^{d'}$, with $d' < d$. The choice made in (4) is only due to simplicity reasons. Note that many conservative or nonconservative problems (in particular, conservation laws and balance laws) are included here; e.g. see [6,8].

Consider, for definiteness, the class of scalar hyperbolic (transport) equations, in space dimension $d \geqslant 1$,

$$u_t + \nabla \cdot f(u) = c(x, t)u + s(x, t), \tag{7}$$

subject to certain initial or initial-boundary data. Here, $x = (x_1, x_2, \ldots, x_d) \in \mathbf{R}^d$, $0 < t < T$, $u = u(x, t)$ and $c(x, t)$ are scalar, $s(x, t)$ is a source term, $f = (f_1, f_2, \ldots, f_d) \in \mathbf{R}^d$, and the appropriate smooth regularity is assumed throughout. Eq. (7) can be rewritten as

$$Lu := u_t + \sum_{i=1}^{d} g_i(u)u_{x_i} - c(x, t)u - s(x, t) = 0, \tag{8}$$

where we set $g_i(u) := f_i'(u)$; g_i, as well as f, might also depend explicitly on time. We shall force the ideally sampled solution, say

$$u^S(x, t) := \sum_{n=1}^{N_T} u(x^n(t), t) \prod_{i=1}^{d} \delta(x_i - x_i^n(t)), \tag{9}$$

where we set $x = x^n(t) \equiv (x_1^n(t), \ldots, x_d^n(t))$, to solve Eq. (8) on characteristics, while the *reconstructed* solution, at time t, is given by

$$u(x, t) = \sum_{n=-\infty}^{+\infty} u(nh, t)sinc\left(\frac{x - nh}{h}\right), \tag{10}$$

being

$$u(nh, t) = \frac{1}{h} \int_{-\infty}^{+\infty} u(x, t)sinc\left(\frac{x - nh}{h}\right)dx, \tag{11}$$

for x in $\mathbf{R}$. In $\mathbf{R}^d$, $d > 1$, we have instead

$$u(x_1, \ldots, x_d, t) = \sum_{k_1, \ldots, k_d = -\infty}^{+\infty} u(k_1 h_1, \ldots, k_d h_d, t) \prod_{i=1}^{d} sinc\left(\frac{x_i - k_i h_i}{h_i}\right), \tag{12}$$

where

$$u(k_1h_1,\ldots,k_dh_d,t)=\frac{1}{h_1\cdots h_d}\int_{\mathbf{R}}\cdots\int_{\mathbf{R}}u(x_1,\ldots,x_d,t)\left(\prod_{i=1}^{d}sinc\left(\frac{x_i-k_ih_i}{h_i}\right)\right)dx_1\cdots dx_d. \tag{13}$$

We have assumed equally spaced interpolation points on each direction, the space step-size being h_i in the direction x_i.

In (9), N_T denotes the maximum number of sampled values used (up to time T); similar results can be obtained if the sample index runs over an interval like $(-N_T,N_T)$, with $N_T\leqslant+\infty$. Let evaluate first

$$\begin{aligned}u_t^S(x,t)&=\frac{\partial}{\partial t}\left[\sum_{n=1}^{N_T}u(x^n(t),t)\prod_{i=1}^{d}\delta(x_i-x_i^n(t))\right]=\sum_{n=1}^{N_T}\left\{\left[\sum_{i=1}^{d}u_{x_i}(x^n(t),t)[(x_i^n(t))'-g_i(u)]+cu+s\right]\prod_{i=1}^{d}\delta(x_i-x_i^n(t))\right.\\&\left.-u(x^n(t),t)\sum_{i=1}^{d}\left(\prod_{j=1\,j\neq i}^{d}\delta(x_j-x_j^n(t))\right)\delta(x_i-x_i^n(t))(x_i^n(t))'\right\},\end{aligned}$$

where we have used (8) to eliminate u_t, $(x_i^n(t))'=dx_i^n(t)/dt$, and u is evaluated at $(x^n(t),t)$;

$$\begin{aligned}u_{x_i}^S(x,t)&=\frac{\partial}{\partial x_i}\left[\sum_{n=1}^{N_T}u(x^n(t),t)\prod_{i=1}^{d}\delta(x_i-x_i^n(t))\right]=\sum_{n=1}^{N_T}u(x^n(t),t)\frac{\partial}{\partial x_i}\left(\prod_{i=1}^{d}\delta(x_i-x_i^n(t))\right)\\&=\sum_{n=1}^{N_T}u(x^n(t),t)\left(\prod_{j=1\,j\neq i}^{d}\delta(x_j-x_j^n(t))\right)\delta'(x_i-x_i^n(t)).\end{aligned}$$

We then obtain

$$\begin{aligned}Lu^S(x,t)&=u_t^S+\sum_{i=1}^{d}g_i(u^S)u_{x_i}^S-cu^S(x,t)-s(x,t)\\&=\sum_{n=1}^{N_T}\left\{\left[\sum_{i=1}^{d}u_{x_i}(x^n(t),t)[(x_i^n)'-g_i(u)]+cu(x,t)+s(x,t)\right]\prod_{i=1}^{d}\delta(x_i-x_i^n(t))\right.\\&\left.-u\sum_{i=1}^{d}(x_i^n)'\delta'(x_i-x_i^n(t))\prod_{j=1,j\neq i}^{d}\delta(x_j-x_j^n(t))+\sum_{i=1}^{d}g_i(u^S)u\delta'(x_i-x_i^n(t))\prod_{j=1,j\neq i}^{d}\delta(x_j-x_j^n(t))\right\}-cu^S(x,t)-s(x,t)\\&=\sum_{n=1}^{N_T}\left\{\left[\sum_{i=1}^{d}u_{x_i}(x^n(t),t)[(x_i^n)'-g_i(u)]+s(x^n(t),t)\right]\prod_{i=1}^{d}\delta(x_i-x_i^n(t))\right.\\&\left.-\sum_{i=1}^{d}[(x_i^n)'-g_i(u^S)]\delta'(x_i-x_i^n(t))\left(\prod_{j=1,j\neq i}^{d}\delta(x_j-x_j^n(t))\right)\right\}-s(x,t).\end{aligned}$$

Again, u and u_{x_i} are evaluated at $(x^n(t),t))$. It is essential here to note that $g_i(u)\equiv g_i(u^S)$, in view of the fact that the (only) argument of the $g_i(u)$'s is the integral $\int_{\mathbf{R}^d}\mathcal{K}(\xi)u(\xi,t)d\xi$, and such an integral takes the same value for u^S given by (9) and u considered expanded in series of *sinc* as in (2), e.g. see [13, Section 2.1]. (We do not discuss here the various classes of functions, such as, for instance, the Paley–Wiener class, to which this kind of interpolation applies.)

Now, equation $Lu^S(x,t)=0$ holds if, for every n, $n=1,2,\ldots,N_T$,

$$\left(\sum_{i=1}^{d}u_{x_i}((x_i^n)'-g_i)\right)\left(\prod_{i=1}^{d}\delta(x_i-x_i^n(t))\right)-u\sum_{i=1}^{d}((x_i^n)'-g_i)\delta'(x_i-x_i^n(t))\prod_{j\neq i}\delta(x_j-x_j^n(t))=0, \tag{14}$$

and to this purpose, the conditions

$$(x_i^n)'=g_i(u(x^n(t),t),\quad i=1,2,\ldots d,\ \ n=1,2,\ldots,N_T. \tag{15}$$

suffice. These are precisely the ODEs defining the *characteristics* of the PDE in (7). After that the characteristics have been obtained, we have from such PDE

$$\left.\frac{du}{dt}\right|_{char.}=\frac{du}{dt}(x^n(t),t)=c(x^n(t),t)u(x^n(t),t)+s(x^n(t),t)),\quad n=1,2,\ldots,N_T. \tag{16}$$

3. Reconstructing the solution at times $t>0$: a Shannon formula for unevenly spaced points in 1D

Even starting from evenly spaced samples, say x_n, at time $t=0$, the sampled values, $x_n(t)$, needed to reconstruct the solution $u(x,t)$ at later times, $t>0$, will be in general *unevenly* spaced. Therefore, the classical, simplest formulation of Shannon theorem cannot be used. Generalizations of Shannon's theorem for such cases have been given in the literature, see, e.g. the Paley–Wiener–Levinson sampling theorem [28]. We prefer to keep the form similar to that in (2) proceeding as follows, circumventing such a difficulty (which is the same encountered when using Fourier series on nonuniform meshes) mapping the

unevenly spaced points onto a uniformly spaced set of points. This task can be accomplished by means of *monotonic* maps, so to preserve the order of points. One of the most effective methods is to construct such a map using a special kind of cubic splines, which do preserve monotonicity (giving up C^2-continuity). A large body of literature has been devoted to such issues, since they have an independent interest. These splines are referred to as "shape preserving" splines, e.g. see [2,3,17,19,26]. The aforementioned map, however, may destroy the property of having a rigorously finite band size, hence some care should be devoted to this point too.

Consider a function, $f(x)$, known at a finite number of *unevenly* spaced points, $x_i,\ i = 1,\dots,N$. Let T be a one-to-one transformation, mapping the x_i's into a set of *evenly* spaced points, ξ_i, and let h be the distance between any two of the ξ_i's, i.e.

$$\xi_i = ih = T(x_i), \quad i = 1,2,\dots,N.$$

If T is differentiable and S denotes the inverse transform of T, we have

$$x_i = S(\xi_i) = S(ih), \quad i = 1,2,\dots,N,$$

and then $|T'(x)| = 1/|S'(\xi)|$, x and ξ being linked by the previous relations. Define the application of f onto the domain of the ξ's as

$$g(\xi) = f(S(\xi)) = f(x),$$

see [19]. We then assume that g is known at the evenly spaced points $\xi_i = ih$ for $i = 1,\dots,N$, and want to reconstruct f on the entire domain.

When $g(\xi)$ is a band-limited function, the Shannon sampling theorem can be used to reconstruct it, and hence to recover $f(x)$,

$$f(x) = \sum_{i=1}^{N} g(ih)\frac{\sin[\pi(T(x)-ih)/h]}{\pi(T(x)-ih)/h} = \sum_{i=1}^{N} g(ih)\,sinc\left(\frac{T(x)-ih}{h}\right)$$

(see (2) with $h = 1/W$). However, the property of $f(x)$ of being band-limited does not guarantee that g also enjoys the same property. Therefore, a modified version of Shannon theorem, taking into account this fact, is required, which is

$$f(x) = |T'(x)| \sum_{i=1}^{N} |S'(ih)|g(ih)\,sinc\left(\frac{T(x)-ih}{h}\right), \tag{17}$$

see [19]. In our method below, the abscissas of the (space) points on which we want to reconstruct "the signal", evolve in time, hence a suitable technique is needed to reconstruct the transformation T at each time, so to pass from unevenly spaced points to evenly spaced points. To this purpose, we construct *monotonic cubic splines*, which preserve the order of points.

To interpolate with monotone cubic splines, we proceed as follows. Given a set (x_i, ξ_i) of points in the (x,ξ) plane, the interpolatory function we construct is on each interval (x_i, x_{i+1}) a third-degree polynomial through the points (x_i, ξ_i) and (x_{i+1}, ξ_{i+1}). The slope at each node is prescribed in such a way to guarantee the monotonicity of the interpolant, termed "a shape preserving cubic spline" [2,3]). The resulting curve is continuous along with its first derivative. Giving up the continuity of the second derivative, the resulting degrees of freedom can be used to impose global monotonicity on the entire interval. The method proposed in this paper does exploit an interpolant that is piecewise cubic and has a monotonic behavior. Such interpolant is stable, that is it depends continuously on data, i.e. small perturbations on data lead to small changes in the interpolant.

4. Examples of the reconstruction method for solving PDEs in 1D

Example 4.1. Consider, as a first elementary example, the linear scalar hyperbolic PDE

$$u_t + (1+x)u_x = 0, \quad x \in \mathbf{R},\ t > 0, \tag{18}$$

in one dimension, subject to the initial condition

$$u(x,0) = u_0(x). \tag{19}$$

The characteristic exiting from x^* is the solution to the Cauchy problem

$$\frac{dx}{dt}(t) = 1 + x(t), \quad x(0) = x^*,$$

and hence is

$$x(t;x^*) = (1+x^*)e^t - 1. \tag{20}$$

On the characteristics, u satisfies the ODE

$$\frac{du}{dt}(x(t;x^*),t) = 0,$$

and hence

$$u(x(t;x^*),t) = u_0(x^*). \tag{21}$$

This suggests a numerical scheme for solving the PDE in (18), as follows:

- a given (arbitrary) space interval, $[x_1, x_2]$, is initially discretized with N (evenly spaced) nodes, say $x_i^*,\ i = 1,\dots,N$;
- the initial data, $u_0(x)$, is sampled at the points x_i^*, i.e. the coefficient

  $$\mu_i = u_0(x_i^*)$$

  is associated to every value x_i^*;
- the initial profile $u_0(x)$ can be represented by means of the basis functions $\mathrm{sinc}\, x$, in view of Shannon theorem (provided that the "signal" $u_0(x)$ is band-limited and we use a sufficiently high number of samples; otherwise, act according to (3), estimating a suitable finite bandwidth);
- the quantities $x_i(t)$ are let evolve, accordingly to the ODEs

  $$\frac{dx_i}{dt} = 1 + x_i,$$

  which are solved numerically, e.g. by a Runge–Kutta method, with the initial data

  $$x_i(0) = x_i^*, \quad i = 1,\dots,N;$$

- at any given time $t > 0$, the "signal" $u(x,t)$ is reconstructed (as a function of x), knowing that the value $\mu_i \equiv u(x_i(t;x_i^*),t) = u_0(x_i^*)$ is assigned to it, at the abscissa $x_i(t)$.

Note that, during their evolution, the $x_i(t)$'s may not remain necessarily evenly spaced (even though they started, at $t = 0$, evenly spaced). Hence, the reconstruction should be carried out using a Shannon formula for unevenly spaced points, see (17), Section 3.

This procedure can be applied to every PDEs like

$$u_t + f(x)u_x = 0, \quad x \in \mathbf{R},\ \ t > 0,$$

for which the evolution of the corresponding $x_i(t)$'s is governed by the system of ODEs

$$\frac{dx_i}{dt} = f(x), \quad i = 1,\dots,N,$$

under the initial conditions $x_i(0) = x_i^*$. Here we give the results obtained applying the method described above to problem (18) and (19).

If $2L$ is the support size of the "signal" and W its *approximate* bandwidth, the minimum number of samples required for this purpose is *approximately* $N_s = 2WL$; clearly, it would be safer to oversample, taking a number of points larger than that. In this example we considered a Lorentzian-type initial profile,

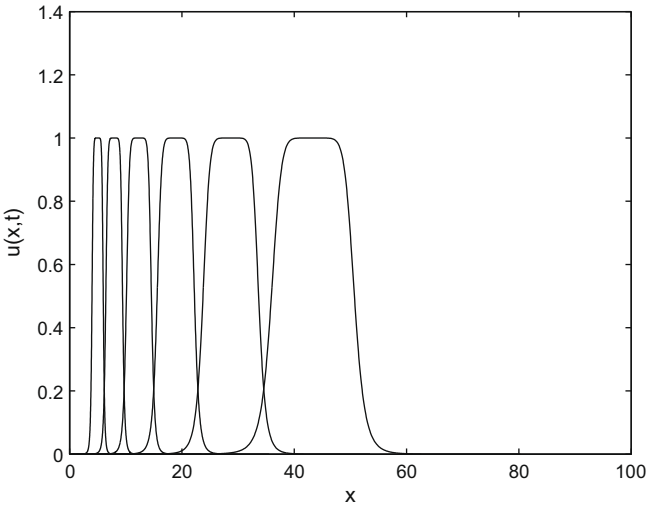

Fig. 1. Profile of $u(x,t)$ of Example 4.1, every 400 iterates.

$$u_0(x) = \frac{1}{1+(x-5)^8}.$$

We used $N = 80$ points to reconstruct the signal, while the minimum number required was 60. We let evolve the $x_i(t)$'s for $t \in [0,2]$. In Fig. 1, the behavior of $u(x,t)$ is shown every 400 iterates (i.e. the solution is plotted at times $t = 0(0.2)2$, having used a time-step $h = 0.001$ in the computations).

Example 4.2. Consider the linear PDE

$$u_t + xu_x + u = 0, \quad x \in \mathbf{R}, \ t > 0, \tag{22}$$

with the initial data

$$u(x,0) \equiv u_0(x) = \frac{1}{1+(x-x_0)^{2m}},$$

for various fixed integers m, whose solution is

$$u(x,t) = \frac{e^{-t}}{1+(xe^{-t}-x_0)^{2m}}.$$

The characteristic stemming from x^* is the solution to the ODE problem

$$\frac{dx}{dt}(t) = x(t), \quad x(0) = x^*,$$

and is thus given by

$$x(t;x^*) = x^* e^t.$$

The solution on the characteristics is obtained solving the ODE

$$\frac{du}{dt}(x(t;x^*),t) = -u,$$

and hence is

$$u(x(t;x^*),t) = u_0(x^*)e^{-t}. \tag{23}$$

We proceed as in Example 4.1. Now the quantities $x_i(t)$'s evolve according to the ODE system

$$\frac{dx_i}{dt} = x_i, \quad x_i(0) = x_i^*, \ i = 1,\dots,N,$$

and at any given time $t > 0$, $u(x,t)$ is reconstructed, knowing that at the abscissa $x_i(t)$ the value $\mu_i(t) \equiv u(x_i(t;x_i^*),t) = u_0(x_i^*)e^{-t}$ is assigned in view of (23). Again, the $x_i(t)$'s, evolving, may not necessarily remain evenly spaced.

The entire procedure can be applied to PDEs like

$$u_t + f(x)u_x + g(x)u = 0, \quad x \in \mathbf{R}, \ t > 0,$$

where the $x_i(t)$'s solve the initial value problem

$$\frac{dx_i}{dt} = f(x_i), \quad x_i(0) = x_i^*, \ i = 1,\dots,N.$$

Then, we solve

$$\frac{du}{dt}(x_i(t),t)) = -g(x_i(t))u(x_i(t),t), \quad i = 1,\dots,N.$$

The solution to such a problem has been computed choosing as initial data the same Lorentzian profile of the previous example. The numerical results have been compared with the analytical solution, as well as with that obtained by a finite difference scheme, see Figs. 2 and 3.

Remark. In [8], an initial-boundary value problem, used to describe crystal precipitation, which presents some pathologies, was solved using the present numerical method. Such problem concerned a nonlinear integro-differential equation (see Example 4.3 below), the unknown representing a crystal size distribution evolving in time. The quantities $x_i(t)$ represent some of the crystal amplitudes, which vanish and hence are dropped out from the problem as time goes on. Consequently, there is a progressive loss of amplitudes, i.e. of samples. This fact reduces the accuracy in the Shannon reconstruction. At some $t > 0$, the number of samples fall below the minimum needed for a full reconstruction, and hence a re-sampling procedure should be implemented. Alternatively, we can start with a sufficiently (initially redundant) higher number of samples. However, in view of Shannon theorem, it is possible to evaluate at every time-step the Fourier transform of the

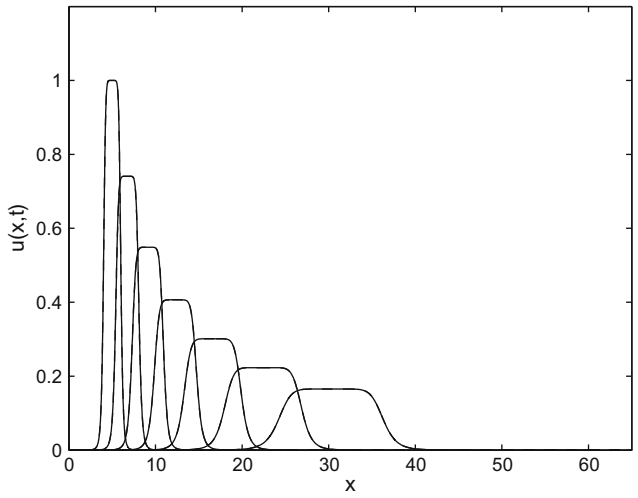

Fig. 2. Comparison between the numerical solution $u(x,t)$ of Example 4.2, obtained by the Shannon sampling method (continuous line) and the analytical solution (dashed line), at various times.

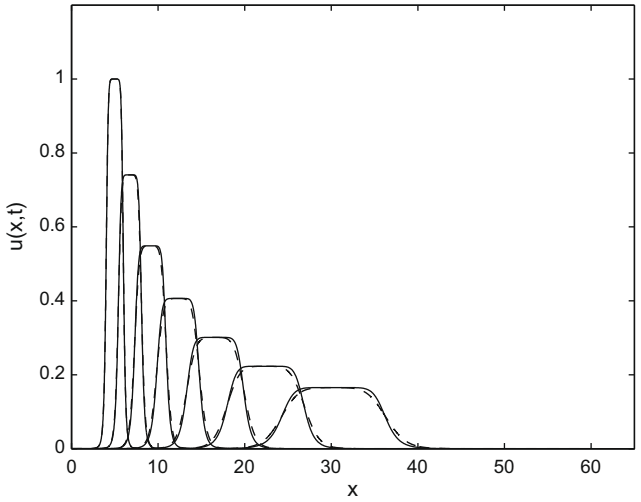

Fig. 3. Comparison between the numerical solution $u(x,t)$ of Example 4.2, obtained by the Shannon sampling method (continuous line) and the solution computed by a finite difference scheme (dashed line), at various times.

solution, and estimate its bandwidth (in general approximately, even because it is necessarily unbounded) and hence decide whether the number of available samples suffices. We refer to [8] for details and figures.

Example 4.3. Consider the *nonlinear* PDE

$$\partial_t u + \partial_x \left(u \int_{-\infty}^{+\infty} u(\xi, t) d\xi \right) = f(x,t), \tag{24}$$

where

$$f(x,t) := -\left(1 + 2\sqrt{\pi} x e^{-t}\right) e^{-(x^2+t)},$$

on the domain $(-\infty, +\infty) \times (0, T]$, $T > 0$ fixed, along with the initial and boundary data

$$u(x,0) = u_0(x) := e^{-x^2}, \quad u(\pm\infty, t) := \lim_{x \to \pm\infty} u(x,t) = 0.$$

Its solution is

$$u(x,t) = e^{-x^2} e^{-t}. \tag{25}$$

The characteristics of the PDE in (24) obey the ODE

$$x'(t) = \int_{-\infty}^{+\infty} u(\xi, t)d\xi, \quad x(0) = x^*,$$

wherefrom

$$x(t) := x(t; x^*) = x^* + \int_0^t ds \int_{-\infty}^{+\infty} u(\xi, t)d\xi. \tag{26}$$

The solution to (24) is therefore given by

$$u(x(t; x^*), t) = u_0(x^*) + \int_0^t f(x(s; x^*), s)ds. \tag{27}$$

The algorithm which implements our Shannon-based method consists of the same steps of Example 4.1:

- Discretize the space interval $[-a, a]$ (for a value of a sufficiently large), with N points, say x_i^*, $i = 1, 2, \ldots, N$.
- Sample the (known) function $u_0(x)$ at the points x_i^*, defining the "weights" $\mu_i := u_0(x_i^*)$.
- Let evolve the positions $x_i(t)$ of the samples according to (26). Here, the space integral has been discretized by Simpson's rule. The calculation is affected by an additional $\mathcal{O}(\Delta t)$ error, since the solution here has been integrated up to time $t - \Delta t$, rather that up to time t.
- Update the coefficients $\mu_i(t)$ according to (27). In particular, we obtain

$$\mu_i(t) = \mu_i(t - \Delta t) + \int_t^{t+\Delta t} f(x(s; x_i^*), s)ds.$$

  This integral is evaluated numerically by the trapezoidal rule.
- The solution is then reconstructed (approximately) by Shannon formula.

Taking, for definiteness, $a = 5,\ N = 500,\ \Delta t = 0.5 \times 10^{-4},\ T = 5$, the number of points on which the solution has been reconstructed is $M = 2000$. In Fig. 4, a comparison is made between the analytical solution, $\tilde{u}$, given in (25), and the numerical solution, at various times. In Table 1, the r.m.s. error,

$$e_2(t) := \left(\sum_{i=1}^{M} [u(x_i, t) - \tilde{u}(x_i, t)]^2 \right)^{1/2}, \tag{28}$$

is shown as a function of the time-step-size, Δt. In Fig. 5, the solution, $u(x, t)$, is plotted at few values of time.

5. The reconstruction method for solving PDEs in 2D and numerical examples of it

We first consider the problem of unevenly spaced samples in two dimensions, and then give some numerical examples.

5.1. Shannon formula for unevenly spaced points in 2D

Let $f(x, y)$ be a function, known at a finite number of unevenly spaced points, $(x_i, y_j),\ i = 1, \ldots, N,\ j = 1, \ldots, M$, and let T be a one-to-one transformation mapping such points onto a set of points $(\bar{x}_i, \bar{y}_j)$, evenly spaced, in each direction, x and y, with steps $\Delta x,\ \Delta y$, respectively, i.e.

$$(\bar{x}_i, \bar{y}_j) = (i\Delta x, j\Delta y) = T(x_i, y_j), \quad i = 1, 2, \ldots N,\ j = 1, 2, \ldots M.$$

If S denote the inverse of T, that is

$$(x_i, y_j) = S(\bar{x}_i, \bar{y}_j) = S(i\Delta x, j\Delta y),$$

we define the application of f onto the domain of the evenly spaced points as

$$g(\bar{x}, \bar{y}) = f(S(\bar{x}, \bar{y})) = f(x, y).$$

Hence, we assume to know g at the evenly spaced points $(\bar{x}_i, \bar{y}_j)$ for $i = 1, \ldots, N$ and $j = 1, \ldots, M$, and want to reconstruct f on the entire domain. The Shannon sampling theorem is used to realize such a task (with the usual restrictions and errors), and hence to recover $f(x, y)$:

$$f(x, y) = \sum_{i=1}^{N} \sum_{j=1}^{M} g(i\Delta x, j\Delta y)\, sinc\left(\frac{\bar{x} - i\Delta x}{\Delta x}\right) sinc\left(\frac{\bar{y} - j\Delta y}{\Delta y}\right). \tag{29}$$

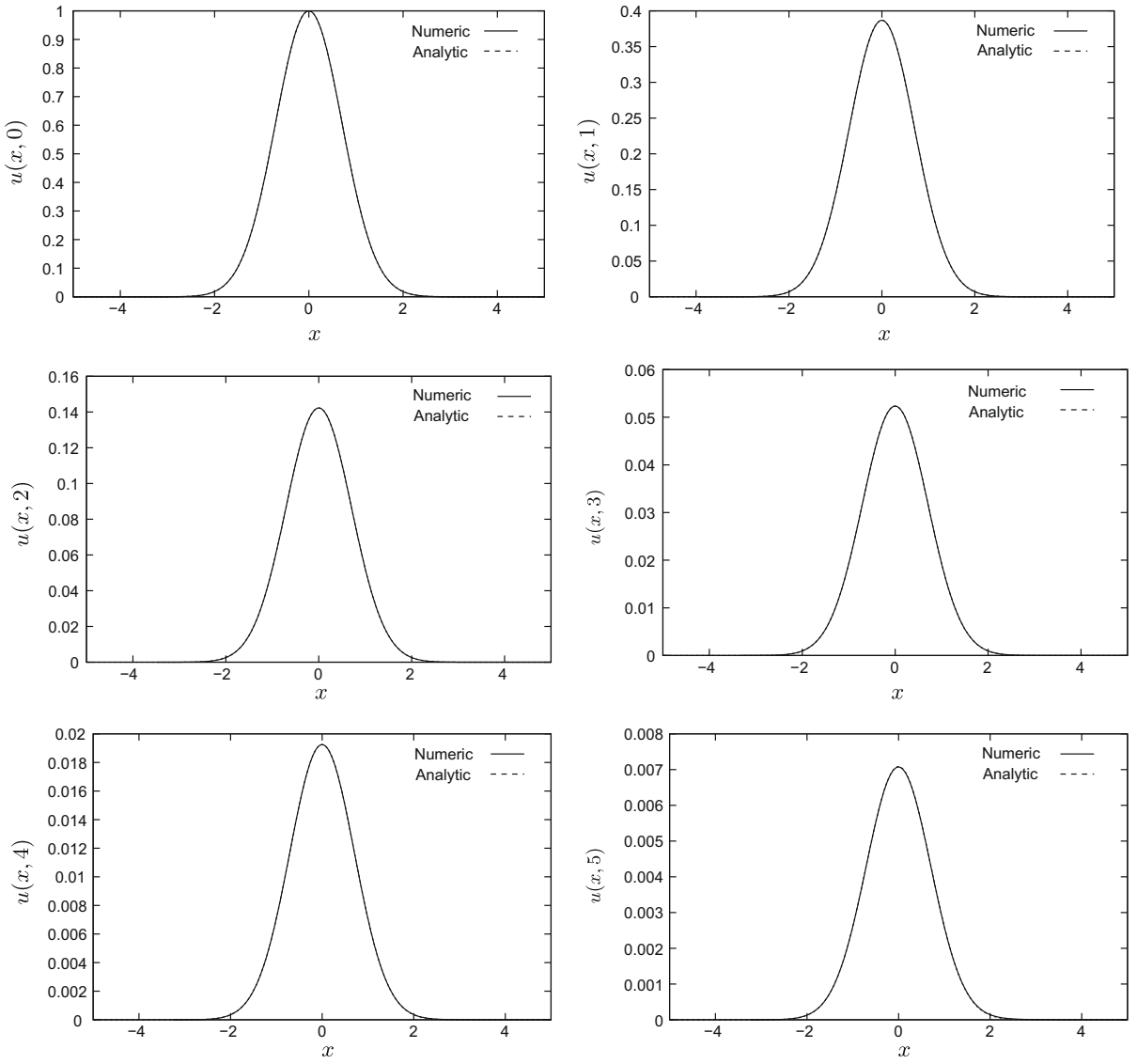

Fig. 4. Comparison between the numerical and the analytical solution in Example 4.3, at various times.

Table 1
Error computed at time $T = 5$ for various time-step-sizes, Δt, in Example 4.3.

Δt	e_2
0.0016	0.0044529
0.0008	0.0022268
0.0004	0.0011135
0.0002	0.0005567
0.0001	0.0002784
0.00005	0.0001392

In the method below, the coordinates of the points on which we want to reconstruct the signal, evolve in time, hence it is necessary to devise a technique to construct at each time the transformation T that allows to map the unevenly spaced points onto evenly spaced points. One can easily show that S is invertible, but its inverse is not easily computable. On the other hand, it is not necessary to know T explicitly. In fact, the relation (29) can be applied when the points $(\bar{x}, \bar{y})$ vary in the evenly spaced domain, then assigning the computed value of f to the point $(x, y) = S(\bar{x}, \bar{y})$. For some information on the sampling theory in several dimensions, see, e.g. [7].

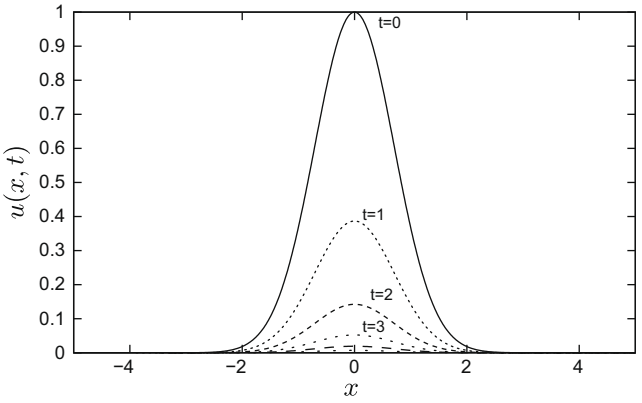

Fig. 5. Profile of solution, $u(x,t)$, in Example 4.3 at various times.

5.2. Numerical examples

Example 5.2.1. Consider the linear PDE

$$u_t + (1+x)u_x + (1+y)u_y = 0, \quad (x,y) \in \mathbf{R}^2, \ \ t > 0, \tag{30}$$

with the initial condition

$$u(x,y,0) = u_0(x,y).$$

This case is the 2D straightforward generalization of the 1D problem in Example 4.1. The characteristic stemming from (x_0,y_0) is the solution to the Cauchy problem

$$\begin{cases} x'(t) = 1 + x(t), & x(0) = x_0 \\ y'(t) = 1 + y(t), & y(0) = y_0, \end{cases}$$

hence

$$x(t;x_0,y_0) \equiv x(t) = (1+x_0)e^t - 1, \quad y(t;x_0,y_0) \equiv y(t) = (1+y_0)e^t - 1.$$

On the characteristics, u satisfies the ODE

$$\frac{du}{dt}(x(t),y(t),t) = 0,$$

and thus

$$u(x(t),y(t),t) = u_0(x_0,y_0). \tag{31}$$

As in the 1D problems, this procedure consists of the following steps:

- a rectangle, $[x_1,x_2] \times [y_1,y_2]$ is discretized with $N \times M$ (evenly spaced) nodes, $(x_i(0),y_j(0)),\ i = 1,\dots,N,\ j = 1,\dots,M$;
- the initial data, $u_0(x,y)$, is sampled at the points $(x_i(0),y_j(0))$, i.e. the coefficient

  $$\mu_i = u_0(x_i(0),y_j(0))$$

  is associated to each point $(x_i(0),y_j(0))$;
- the surface $u_0(x,y)$ (it is nice to have a geometrical picture) is constructed by means of the basis functions $sinc(x)sinc(y)$, in view of Shannon theorem;
- the points $(x_i(t),y_j(t))$ are let evolve according to the system of ODEs

  $$\begin{cases} \frac{dx_i}{dt} = 1 + x_i \\ \frac{dy_j}{dt} = 1 + y_j, \end{cases}$$

  with the initial data $x_i(0),\ y_j(0),\ i = 1,\dots,N,\ j = 1,\dots,M$, and such a system is solved numerically, e.g. by an explicit 4th-order Runge-Kutta method (a TVD 3rd-order Runge–Kutta method [9,27] was also used, showing negligible discrepancies);
- at each fixed time $t > 0$, "the signal" $u(x,y,t)$ can be reconstructed (with the usual restrictions), knowing that the value $\mu_i \equiv u(x_i(t),y_j(t),t) = u_0(x_i(0),y_j(0))$ is assigned to the point $(x_i(t),y_j(t))$.

As in the one-dimensional problems, when the points $(x_i(t), y_j(t))$ evolve, in general they do not remain evenly spaced, even though they may have started evenly spaced. For such a reason, the reconstruction should be carried out using a Shannon formula for unevenly spaced points.

The full procedure can be repeated to handle the more general class of PDEs

$$u_t + f(x,y)u_x + g(x,y)u_y = 0, \quad (x,y) \in \mathbf{R}^2, \ t > 0,$$

for which the evolution of the points $(x_i(t), y_j(t))$ is governed by the system

$$\begin{cases} \frac{dx_i}{dt} = f(x,y), & i = 1, \dots, N, \\ \frac{dy_j}{dt} = g(x,y), & j = 1, \dots, M, \end{cases}$$

with the initial conditions $x_i(0), y_j(0)$. Here we display the results obtained applying the method to the problem (30). In such example, we considered a Lorentzian initial profile

$$u_0(x,y) = \frac{1}{1+(x-5)^8} \frac{1}{1+(y-5)^8},$$

and used $N \times M = 80 \times 80$ points to sample the signal. The quantities $(x_i(t), y_j(t))$ were let evolve for $t \in [0,2]$. In Fig. 6, we show $u(x,y,t)$ at times $t = 0$ and $t = 2$. Note that when time goes on, the initial profile is translated but keeps its shape as well as its maximum value, see (31).

Example 5.2.2. The linear PDE

$$u_t + xu_x + yu_y + u = 0, \quad (x,y) \in \mathbf{R}^2, \ t > 0, \tag{32}$$

subject to the initial data

$$u(x,y,0) \equiv u_0(x,y) = \frac{1}{1+(x-x_0)^{2m}} \frac{1}{1+(y-y_0)^{2m}},$$

has the solution

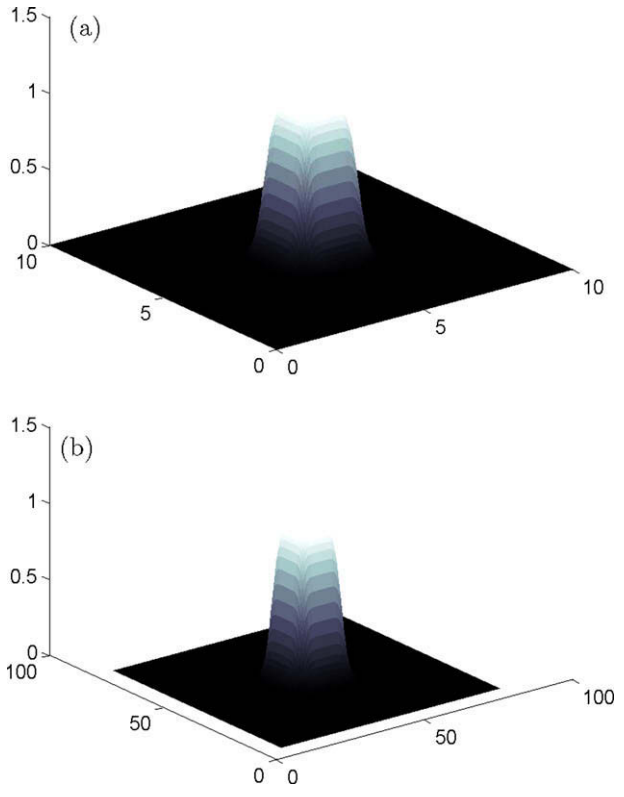

Fig. 6. Profile $u(x,y,t)$ of Example 5.2.1. (a) $t = 0$ and (b) $t = 2$.

$$u(x,y,t) = \frac{e^{-t}}{[1+(xe^{-t}-x_0)^{2m}][1+(ye^{-t}-y_0)^{2m}]}.$$

The equations for its characteristics stemming from (x_0, y_0) are

$$\begin{cases} x'(t) = x(t), & x(0) = x_0, \\ y'(t) = y(t), & y(0) = y_0, \end{cases}$$

and hence

$$x(t;x_0,y_0) \equiv x(t) = x_0 e^t, \quad y(t;x_0,y_0) \equiv y(t) = y_0 e^t.$$

The solution of the PDE on the characteristics is obtained solving the ODE

$$\frac{du}{dt}(x(t),y(t),t) = -u,$$

hence

$$u(x(t),y(t),t) = u_0(x_0,y_0)e^{-t}. \tag{33}$$

The same procedure followed in Example 5.2.2 leads to the system

$$\begin{cases} \frac{dx_i}{dt} = x_i, \\ \frac{dy_j}{dt} = y_j, \end{cases}$$

with initial data $x_i(0),\ y_j(0),\ i = 1,\dots,N$ and $j = 1,\dots,M$, that can be solved, again, e.g. by a Runge–Kutta method. Then, at each time $t > 0$, $u(x,y,t)$ can be reconstructed, knowing the value $\mu_i(t) \equiv u(x_i(t),y_j(t),t) = u_0(x_i(0),y_j(0))e^{-t}$ assigned to the point $(x_i(t),y_j(t))$, see (33). As usual, the points will be in general unevenly spaced.

We applied this method, using the same Lorentzian profile used above as initial data in the previous example, and compare the so-computed solution with the analytical solution, see Fig. 7 for $t = 2$.

Example 5.2.3. The procedure described in the previous example, can be applied to the class of PDEs

$$u_t + f(x,y)u_x + g(x,y)u_y + h(x,y)u = 0, \quad (x,y) \in \mathbf{R}^2, \ t > 0,$$

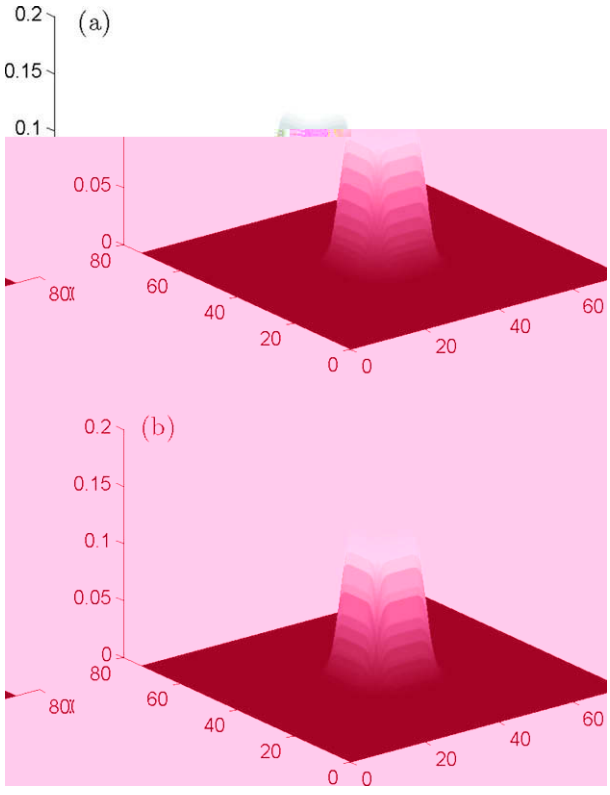

Fig. 7. Comparison between $u(x,y,t)$ and the analytical solution at time $t = 2$ in Example 5.2.2. (a) Numerical solution and (b) analytical solution.

where the evolution of the $(x_i(t), y_j(t))$'s is obtained solving the system of ODEs

$$\begin{cases} \frac{dx_i}{dt} = f(x,y), & i = 1,\dots,N, \\ \frac{dy_j}{dt} = g(x,y), & j = 1,\dots,M, \end{cases}$$

with the initial conditions $x_i(0),\ y_j(0)$. Let summarize the method for this more general class of PDEs. Consider a numerical domain $[x_1,x_2]\times[y_1,y_2]$, discretized with $N\times M$ (evenly spaced) nodes $(x_i(0),y_j(0))$ for $i=1,\dots,N$ and $j=1,\dots,M$. The initial data $u_0(x,y)$ is evaluated at the discrete points of this lattice, so that the following set of coefficients associated to the lattice nodes are defined as

$$\mu_{ij} = u_0(x_i(0), y_j(0)).$$

The time evolution of the point coordinates $(x_i(t), y_j(t))$ is described by the ODEs system above with the initial data $(x_i(0), y_j(0))$. This system is solved numerically by a suitable algorithm, such as the 4th order Runga-Kutta scheme (as we did in our examples).

Along the characteristics u satisfies the ODE

$$\frac{du(x(t),y(t);t)}{dt} = -h(x(t),y(t))u(x(t),y(t);t),$$

from which we obtain

$$u(x(t),y(t);t) = u_0(x(0),y(0);0)\exp\left(-\int_0^t h(x(s),y(s)))ds\right). \tag{34}$$

From (34), we approximate the time evolution of the coefficients $\mu_{ij}(t) = u(x(t),y(t);t)$. In particular, the coefficients $\mu_{ij}(t)$ at time t are given by\

$$\mu_{ij}(t) = \mu_{ij}(0)\exp\left(-\int_0^t h(x_i(s),y_j(s))ds\right), \quad i=1,\dots,N, \quad j=1,\dots,M,$$

where the integral is evaluated numerically by the trapezoidal rule.

Finally, at each time t, the solution $u(x,y,t)$ can be reconstructed by the Shannon formula (29) (for unevenly spaced points), where each discrete point $(x_i(t),y_j(t))$ is associated to its corresponding weight $\mu_{ij}(t)$.

As a specific example of this class of PDEs, we considered the PDE

$$u_t + (x+y)u_x + (x+y)u_y + u = 0, \quad (x,y)\in\mathbf{R}^2,\ \ t>0.$$

The points $(x_i(t),y_j(t))$ evolve in such a way that the shape of the domain does not remain rectangular. Our method keeps track of the deformation of the domain, and is capable nevertheless to reconstruct the solution correctly. In Fig. 8, the solution is shown at $t=0$ and at $t=2$.

Example 5.2.4. Applying our method to the linear PDE

$$u_t + x^2u_x + y^2u_y + 2(x+y)u = 0, \quad (x,y)\in[0,1]\times[0,1],\ \ t>0, \tag{35}$$

with the initial data

$$u(x,y,0)\equiv u_0(x,y) = \sin(\pi x)\sin(\pi y), \quad (x,y)\in[0,1]\times[0,1],$$

we get for the characteristic exiting from (x_0,y_0) the system

$$\begin{cases} x'(t) = x^2(t), & x(0) = x_0 \\ y'(t) = y^2(t), & y(0) = y_0. \end{cases}$$

and hence

$$x(t;x_0,y_0)\equiv x(t) = \frac{x_0}{1-x_0t}, \quad y(t;x_0,y_0)\equiv y(t) = \frac{y_0}{1-y_0t}.$$

The solution on the characteristics can be computed solving the ODE

$$\frac{du}{dt}(x(t),y(t),t) = -2(x+y)u,$$

for $(x,y)\in\mathbf{R}^2,\ t>0$, so that

$$u(x(t),y(t),t) = u_0(x_0,y_0)\exp\left\{-2\int_0^t (x(s)+y(s))ds\right\}. \tag{36}$$

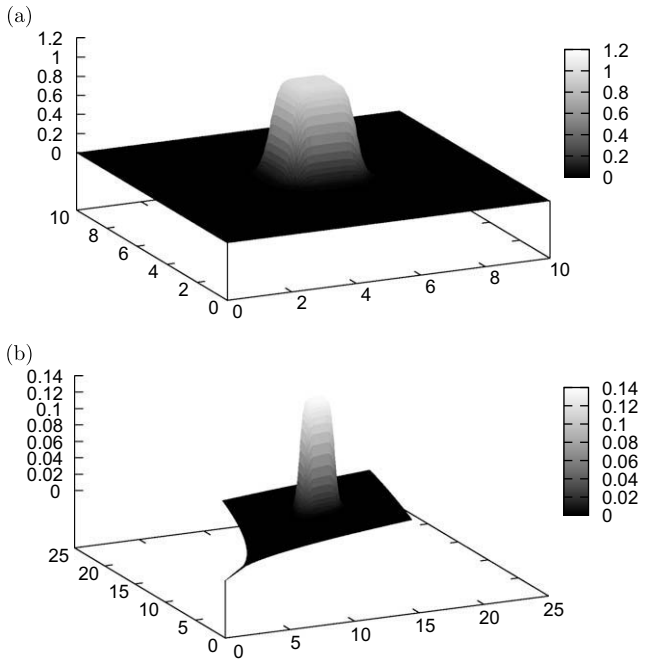

Fig. 8. Profile $u(x,y,t)$ of Example 5.2.3. (a) $t=0$ and (b) $t=2$.

Proceeding as above, we should first solve numerically the ODEs system

$$\begin{cases} \frac{dx_i}{dt} = x_i^2, \\ \frac{dy_j}{dt} = y_j^2, \end{cases}$$

with initial data $x_i(0),\ y_j(0)$, for $i=1,\dots,N$ and $j=1,\dots,M$, and then evaluate $u(x,y,t)$ at each time $t>0$ as

$$u(x_i(t),y_j(t),t) = u_0(x_i(0),y_j(0))\exp\left\{-2\int_0^t (x(s)+y(s))ds\right\},$$

in view of (36). The integral can be evaluated by a quadrature formula, stopping the calculations to the previous time-step, hence introducing a time shift of $\mathcal{O}(\Delta t)$ in computing the solution. In Fig. 9, the solution is shown at times $t=0$ and $t=0.5$.

Example 5.2.5. The two-dimensional analogue of Example 4.3, is the *nonlinear* PDE

$$\partial_t u + \partial_x\left(u\int_{-\infty}^{+\infty}\int_{-\infty}^{+\infty} u(\xi,\eta,t)d\xi\,d\eta\right) + \partial_y\left(u\int_{-\infty}^{+\infty}\int_{-\infty}^{+\infty} u(\xi,\eta,t)d\xi\,d\eta\right) = f(x,y,t), \tag{37}$$

where

$$f(x,y,t) := -\left(1+2\pi(x+y)e^{-t}\right)e^{-(x^2+y^2+t)},$$

on the domain $\mathbf{R}^2\times(0,T]$, with the initial and boundary conditions

$$u(x,y,0) = u_0(x,y) := e^{-(x^2+y^2)}.$$
$$u(\pm\infty,y,t) := \lim_{x\to\pm\infty} u(x,y,t) = 0, \quad u(x,\pm\infty,t) := \lim_{y\to\pm\infty} u(x,y,t) = 0,$$

The solution is

$$u(x,y,t) = e^{-(x^2+y^2)}e^{-t}.$$

The characteristic curves through the point (x^*,y^*) are promptly obtained,

$$x(t) := x(t;x^*) = x^* + \int_0^t\left(\int_{-\infty}^{+\infty}\int_{-\infty}^{+\infty} u(\xi,\eta,t)d\xi\,d\eta\right)dt,$$
$$y(t) := y(t;y^*) = y^* + \int_0^t\left(\int_{-\infty}^{+\infty}\int_{-\infty}^{+\infty} u(\xi,\eta,t)d\xi\,d\eta\right)dt,$$

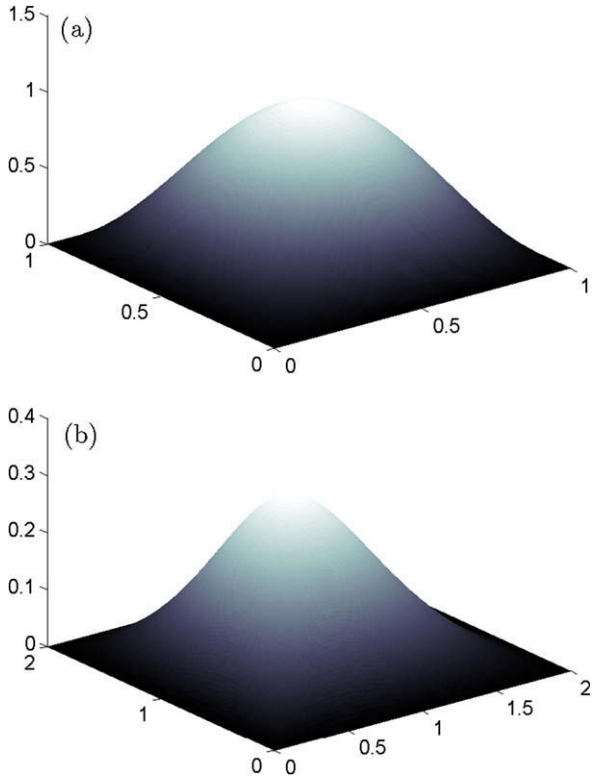

Fig. 9. Profile $u(x,y,t)$ of Example 5.2.4. (a) $t = 0$ and (b) $t = 0.5$.

hence the solution to Eq. (37) on the characteristics is

$$u(x(t;x^*),y(t;y^*),t) = u_0(x^*,y^*) + \int_0^t f(x(s;x^*),y(s;y^*)ds. \tag{38}$$

Our algorithm can be implemented as in Example 4.3. The space domain considered here has been truncated to $[-a,a]\times[-b,b]$, with $a = b = 5$, and the other parameters are $N_x = N_y = 500$, $\Delta t = 0.5\times 10^{-4}$, and $T = 1$. The solution has been reconstructed on $M = 1000$ points. In Fig. 10 the surface-solution is shown at times $t = 0.5$ and $t = 1$.

6. The case of systems of PDEs

Our method can be applied directly to *systems* of hyperbolic equations that admits of characteristics, but may also be applied in some other cases. Below, we give some numerical examples.

6.1. The general method

It is possible to apply our approach even to some systems which do not admit of characteristics, proceeding as follows. Consider the following system of two coupled transport (hyperbolic) equations,

$$\begin{cases} \partial_t u_1 + \sigma_1(x)\partial_x u_1 + f_1(x,u_1,u_2,\partial_x u_2) = 0, \\ \partial_t u_2 + \sigma_2(x)\partial_x u_2 + f_2(x,u_1,u_2,\partial_x u_1) = 0, \end{cases} \tag{39}$$

satisfied by $u_1 \equiv u_1(x,t)$ and $u_2 \equiv u_2(x,t)$. We can apply our method, which is based on the existence of characteristics, to each one of such equations, considering u_2 known in the first equation and u_1 known in the second one. In particular, the characteristic of the first equation stemming from x_1^* is given by the solution, $x_1(t;x_1^*)$, of the Cauchy problem

$$\begin{cases} x_1' = \sigma_1(x_1), \\ x_1(0) = x_1^*. \end{cases} \tag{40}$$

Similarly, we obtain from the second equation in (39)

$$\begin{cases} x_2' = \sigma_2(x_2), \\ x_2(0) = x_2^*, \end{cases} \tag{41}$$

which yields the characteristic curve, $x_2(t;x_2^*)$, of the second equation.

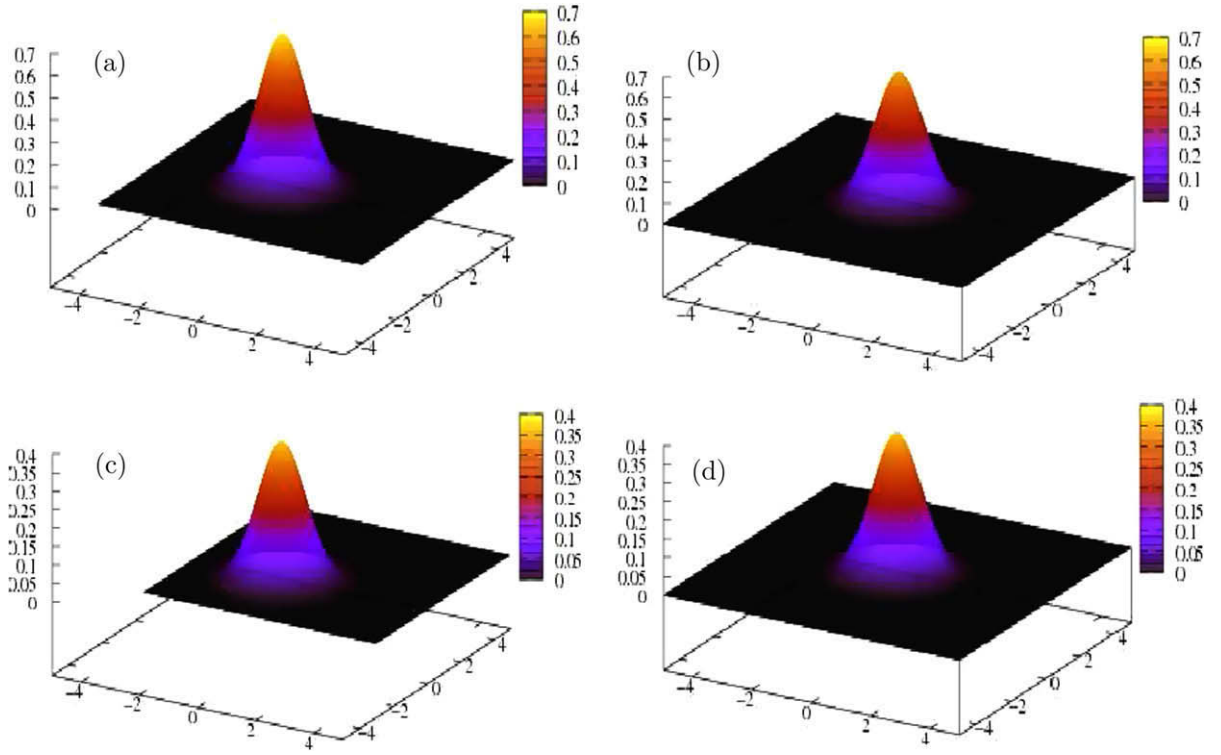

Fig. 10. Comparison between the numerical and the analytical solution in Example 5.2.5, at time $t = 1$: (a) Numerical solution at time $t = 0.5$; (b) analytical solution at time $t = 0.5$; (c) numerical solution at time $t = 1$ and (d) analytical solution at time $t = 1$.

Now, the functions $u_1,\ u_2$ satisfy, each on its own characteristics, the equation

$$\frac{du_{1,2}}{dt}(x_{1,2}(t),t) = \frac{\partial u_{1,2}}{\partial t} + \frac{\partial u_{1,2}}{\partial x}\sigma_{1,2}(x_{1,2}(t)) = -f_{1,2}(x_{1,2}(t), u_1, u_2, \partial_x u_{2,1}),$$

wherefrom

$$u_{1,2}(x_{1,2}(t),t) = u^0_{1,2}(x^*_{1,2}) - \int_0^t f_{1,2}(x_{1,2}(s), u_1, u_2, \partial_x u_{2,1})ds.$$

The idea now is to exploit the Shannon sampling method in both equations, proceeding as in Example 4.1. In the case of systems of two PDEs like (39), our algorithm can be applied to each of the them, as follows. The set of points, x^*_{1i}, x^*_{2i}, given initially (and which initially may even coincide), evolve according to different dynamics. In particular, the evolution of the points x^*_{1i} is governed by the solution of the Cauchy problem (40), while that of the x^*_{2i}'s depend on the solution of (41). This implies some complications in updating the coefficients $u_{1i},\ u_{2i}$, which are given by

$$\begin{aligned} u_{1i} &\equiv u_1(x_{1i}(t;x^*_{1i}),t) = u^0_1(x^*_{1i}) - \int_0^t f_1(x_{1i}(s), u_1, u_2, \partial_x u_2)ds, \\ u_{2i} &\equiv u_2(x_{2i}(t;x^*_{2i}),t) = u^0_2(x^*_{2i}) - \int_0^t f_2(x_{2i}(s), u_1, u_2, \partial_x u_1)ds. \end{aligned} \tag{42}$$

In fact, in the integral term for u_{1i} [u_{2i}], the quantities u_2 and $\partial_x u_2$ [u_1 and $\partial_x u_1$] appear. It is therefore necessary to evaluate u_2 and $\partial_x u_2$ on the characteristics of u_1, and conversely. The values of u_2 at the points x_{1i} can be reconstructed by Shannon formula. Similarly, we proceed to evaluate u_1 at the points x_{2i}. Computing $\partial_x u_2$ at x_{1i} (as well as $\partial_x u_1$ at the x_{2i}'s) requires instead reconstructing u_2 on a fine mesh and then using finite differences at x_{1i} [at x_{2i}]. Note that the quantities x_{1i} and x_{2i}, even if they possibly started from the same values, will in general evolve in a different way. Hence, they might not cover the same space interval, at a given time $t > 0$.

Now, u_2 [u_1] is computed at the points x_{1i} [x_{2i}], but it is known at the points x_{2i} [x_{1i}], and can be reconstructed in the interval $[x_{2min}, x_{2max}]$ (respectively, $[x_{1min}, x_{1max}]$). It follows that it is necessary to check that the two intervals do not depart beyond some given tolerance. When this would happen, the endpoints of such intervals should be redefined so as to coincide adding some points to the left and/or to the right where necessary.

6.2. Numerical examples of the reconstruction method for systems of PDEs

In this subsection we give some numerical results, obtained applying our method to systems of PDEs, and compare them with those obtained by finite difference schemes.

Example 6.2.1. Consider the system

$$\begin{cases} \partial_t u_1 - (1+x)\partial_x u_1 = -u_2, \\ \partial_t u_2 - x\partial_x u_2 = -u_1, \qquad x \in \mathbf{R}, \ \ t > 0. \end{cases}$$

From the first equation we derive the following Cauchy problem, which prescribes the evolution of the characteristics $x_{1i}(t)$,

$$\begin{cases} x'_{1i}(t) = -(1 + x_{1i}(t)), \\ x_{1i}(0) = x^*_{1i}, \end{cases}$$

wherefrom

$$\frac{d}{dt} u_1(x_{1i}(t), t) = -u_2(x_{1i}(t), t),$$

and hence

$$u_1(x_{1i}(t), t) = u_1^0(x^*_{1i}) - \int_0^t u_2(x_{1i}(s), s) ds.$$

Similarly, from the second equation it is the Cauchy problem

$$\begin{cases} x'_{2i}(t) = -x_{2i}(t), \\ x_{2i}(0) = x^*_{2i}, \end{cases}$$

which governs the evolution of the characteristics $x_{2i}(t)$, from which

$$\frac{d}{dt} u_2(x_{2i}(t), t) = -u_1(x_{2i}(t), t),$$

and thus

$$u_2(x_{2i}(t), t) = u_2^0(x^*_{2i}) - \int_0^t u_1(x_{2i}(s), s) ds.$$

Consider the initial profiles

$$u_1^0(x) = u_2^0(x) = \frac{1}{1 + (x - \mu)^8},$$

and choose $[x_{min}, x_{max}] = [0, 10]$ and $\mu = 5$. We discretize this interval with 80 equally distributed nodes, and proceed to the reconstruction on 500 points. Let $h = 0.001$ be the time-step used in the numerical scheme which solves the Cauchy problems.

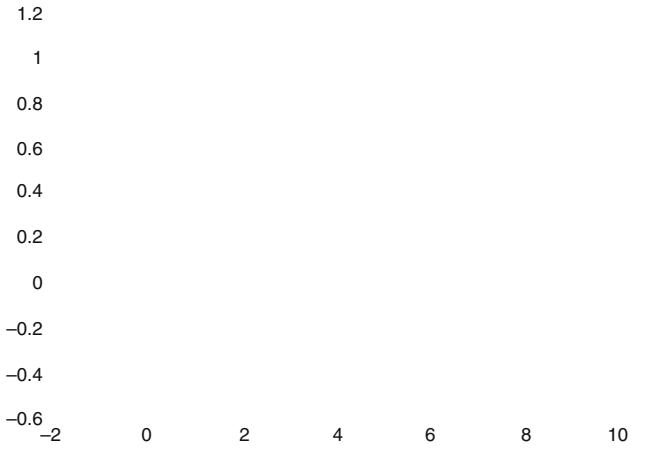

Fig. 11. Example 6.2.1: Comparison between $u_1(x, t)$ given by the Shannon method (continuous line) and obtained by a finite difference scheme (dotted line).

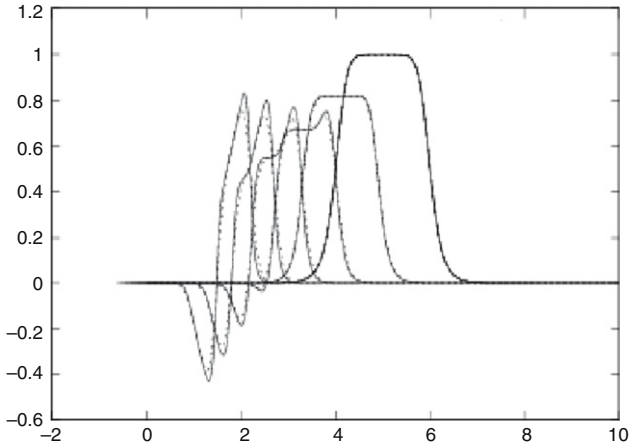

Fig. 12. Example 6.2.1: Comparison between $u_2(x,t)$ given by Shannon's method (continuous line) and that obtained by a finite difference scheme (dotted line).

In Fig. 11 a few profiles of $u_1(x,t)$ are shown, drawn every 400 iterates and compared with those obtained by an explicit finite difference scheme. The corresponding comparison for u_2 is shown in Fig. 12. Note that the departure of solutions is especially pronounced on the peaks. One may conjecture that such peaks are captured more accurately by Shannon's method, since it is not diffusive, hence not dissipative, other than the finite difference scheme.

Example 6.2.2. Consider the system

$$\begin{cases} \partial_t u_1 + \partial_x(u_1 u_2) = 0, \\ \partial_t u_2 - x\partial_x u_2 = -u_1, \qquad x \in \mathbf{R},\ \ t > 0. \end{cases}$$

From the first equation we have the Cauchy problem

$$\begin{cases} x'_{1i}(t) = u_2(x_{1i}(t), t), \\ x_{1i}(0) = x^*_{1i}, \end{cases}$$

which prescribes the characteristics $x_{1i}(t)$, thus

$$\frac{d}{dt} u_1(x_{1i}(t), t) = -u_1(x_{1i}(t), t)\partial_x u_2(x_{1i}(t), t),$$

and hence

$$u_1(x_{1i}(t), t) = u_1^0(x^*_{1i}) \exp\left(-\int_0^t \partial_x u_2(x_{1i}(s), s) ds \right).$$

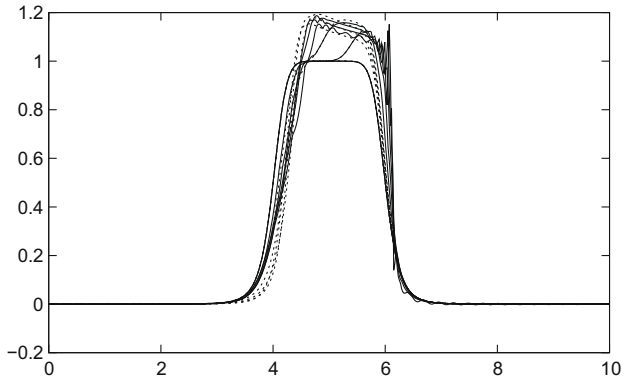

Fig. 13. Example 6.2.2: Comparison between $u_1(x,t)$ computed by Shannon's method (continuous line) and obtained by a finite difference scheme (dotted line).

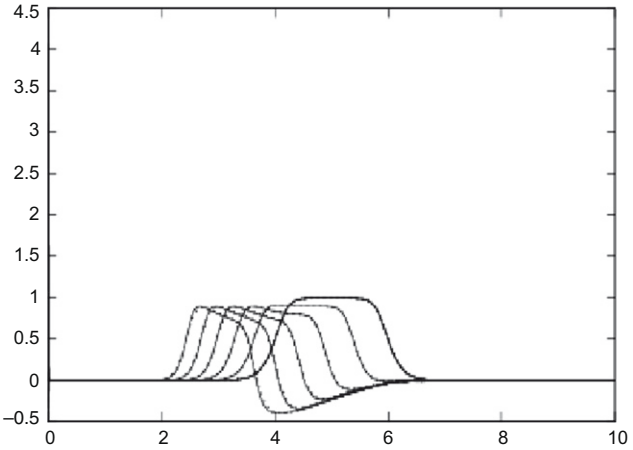

Fig. 14. Example 6.2.2: Comparison between $u_2(x,t)$ computed by Shannon's method (continuous line) and obtained by finite differences (dotted line).

Similarly, from the second equation we derive the Cauchy problem

$$\begin{cases} x'_{2i}(t) = -x_{2i}(t), \\ x_{2i}(0) = x^*_{2i}, \end{cases}$$

which prescribes the evolution of the characteristics $x_{2i}(t)$, thus

$$\frac{d}{dt}u_2(x_{2i}(t),t) = -u_1(x_{2i}(t),t),$$

wherefrom

$$u_2(x_{2i}(t),t) = u_2^0(x^*_{2i}) - \int_0^t u_1(x_{2i}(s),s)ds.$$

We considered the same initial profiles and parameters of the previous example, but stopped the simulation at the 508th iterate, since the characteristics of u_1 cross each other. This spoils the profile of u_1 and, consequently, that of u_2 too. Results are shown in Figs. 13 and 14.

7. Summary

A new method, based on the existence of characteristics, and for this reason essentially *non-dissipative*, is developed, to solve numerically certain single scalar transport (hyperbolic) partial differential equations with smooth solutions, in any dimension. It should be observed that, when applied to linear or semilinear hyperbolic PDEs, in arbitrary dimension, methods based on characteristics are parallelizable. The main idea here rests on sampling the initial profile and letting evolve the so-obtained "samples" along the characteristics. The solution can be reconstructed at any subsequent time, exploiting the Shannon sampling theorem. Shannon's theorem allows to estimate the minimum number of samples with which the full solution can be reconstructed, in principle without any interpolation error. A variety of errors, extensively analyzed in the literature, however occur, and this can be taken into account. The existence of a recently found "fast *sinc* transform" may also play an important role. A number of numerical examples are given to illustrate this approach.

Acknowledgments

This work was supported, in part, by the GNFM of the Italian INdAM.

References

[1] P.L. Butzer, R.L. Stens, Sampling theory for not necessarily band-limited functions: a historical overview, SIAM Rev. 34 (1) (1992) 40–53.
[2] P. Costantini, C. Manni, Monotonicity-preserving interpolation of nongridded data, Comput. Aided Geom. Des. 13 (1996) 467–495.
[3] P. Costantini, C. Manni, Comonotone parametric C^1 interpolation of nongridded data, J. Comput. Appl. Math. 75 (1996) 147–169.
[4] I. Daubechies, R. DeVore, Approximating a bandlimited function using very coarsely quantized data: a family of stable sigma-delta modulators of arbitrary order, Ann. Math. 158 (2003) 679–710.
[5] Ch.-J. De la Vallée Poussin, Sur la convergence des formules d'interpolation entre ordonnées équidistantes, Bull. Cl. Sci. Acad. Roy. Belg. 4 (1908) 319–410.
[6] A. Friedman, B. Ou, D. Ross, Crystal precipitation with discrete initial data, J. Math. Anal. Appl. 137 (1989) 576–590.
[7] A.G. García, Orthogonal sampling formulas: a unified approach, SIAM Rev. 42 (3) (2000) 499–512.

[8] R. Gobbi, S. Palpacelli, R. Spigler, Numerical treatment of a nonlinear nonlocal transport equation modeling crystal precipitation, Math. Models Methods Appl. Sci. 18 (9) (2008) 1505–1527. see also Erratum, Math. Models Methods Appl. Sci. 20, No. 2 (2010).
[9] S. Gottlieb, Chi-Wang Shu, Total variation diminishing Runge–Kutta schemes, Math. Comput. 67 (1998) 73–85.
[10] L. Greengard, J.-Y. Lee, S. Inati, The fast sinc transform and image reconstruction from nonuniform samples in *k*-space, Commun. Appl. Math. Comput. Sci. 1 (2006) 121–131.
[11] A.J. Jerri, The Shannon sampling theorem – its various extensions and applications: a tutorial review, Proc. IEEE 65 (11) (1977) 1565–1596.
[12] V.A. Kotel'nikov, On the carrying capacity of the "ether" and wire in telecommunications, Material for the First All-Union Conference on Questions of Communications, Izd. Red. Upr. Svyazi RKKA, Moscow, 1933.
[13] J. Lund, K.L. Bowers, Sinc Methods for Quadrature and Differential Equations, SIAM, Philadelphia, 1992.
[14] J. McNamee, F. Stenger, E.L. Whitney, Whittaker's cardinal function in retrospect, Math. Comput. 25 (113) (1971) 141–154.
[15] A. Papoulis, Error analysis in sampling theory, Proc. IEEE 54 (7) (1966) 947–955.
[16] C.E. Shannon, A mathematical theory of communication, Bell Syst. Tech. J. 27 (1948) 379–423. and 623–656; Communication in the presence of noise, Proc. IRE 37 (1949) 10–21.
[17] M. Soumek, Band-limited interpolation from unevenly spaced sampled data, IEEE Trans. Acoust. Signal Process. 36 (1) (1988) 110–122.
[18] Stankovic, R.S., Astola, J.T., Karpovsky, M.G., Some historical remarks on sampling theorem, in: J. Astola et al. (Eds.), Proceedings of the 2006 International TICSP Workshop on Spectral Methods and Multirate Signal Processing, SMMSP2006, Florence, Italy, 2–3 September, 2006. TICSP Series, vol. 34, 2006, pp. 163–170.
[19] M. Steffen, A simple method for monotonic interpolation in one dimension, Astron. Astrophys. 239 (1990) 443–450.
[20] F. Stenger, Approximations via Whittaker's cardinal function, J. Approx. Theory 17 (3) (1976) 2222–2240.
[21] F. Stenger, A "sinc-Galerkin" method of solution of boundary value problems, Math. Comput. 33 (145) (1979) 85–109.
[22] F. Stenger, Numerical methods based on sinc and analytic functions, Springer Series in Computational Mathematics, vol. 20, Springer, New York, 1993.
[23] F. Stenger, Numerical methods based on Whittaker cardinal, or sinc functions, SIAM Rev. 23 (2) (1981) 165–224.
[24] J.B. Thomas, B. Liu, Error problems in sampling representations, IEEE Int. Conv. Rec. (USA) 12 (5) (1964) 269–277.
[25] E.T. Whittaker, On the functions which are represented by the expansions of the interpolatory theory, Proc. Roy. Soc. Edinburgh 35 (1915) 181–194.
[26] G. Wolberg, I. Alfy, Monotonic cubic spline interpolation, Computer Graphics Int., 1999, Proceedings of the IEEE, 7–11 June 1999, pp. 188–195.
[27] Y.H. Zahran, A central WENO-TVD scheme for hyperbolic conservation laws, Novi Sad J. Math. 36 (2006) 25–42.
[28] A.I. Zayed, Advances in Shannon's Sampling Theory, CRC Press, Boca Raton, FL, 1993.